Rotational spectroscopy of the isotopic species of silicon monosulphide, SiS

H. S. P. Müller,[*,a,b] M. C. McCarthy,[c,d] L. Bizzocchi,[e] H. Gupta,[c,d,f]
S. Esser,[g] H. Lichau,[a] M. Caris,[a] F. Lewen,[a] J. Hahn,[g]
C. Degli Esposti,[e] S. Schlemmer[a] and P. Thaddeus[c,d]

[a] I. Physikalisches Institut, Universität zu Köln, Zülpicher Str. 77,
50937 Köln, Germany. E-mail: hspm@ph1.uni-koeln.de

[b] Max-Planck-Institut für Radioastronomie, Auf dem Hügel 69,
53121 Bonn, Germany.

[c] Harvard-Smithsonian Center for Astrophysics,
Cambridge, MA 02138, USA,

[d] Division of Engineering and Applied Sciences, Harvard University,
Cambridge, MA 02138, USA

[e] Dipartimento di Chimica 'G. Ciamician', Università di Bologna,
Via F. Selmi 2, 40126 Bologna, Italy

[f] Institute for Theoretical Chemistry, Departments of
Chemistry and Biochemistry, The University of Texas
at Austin, Austin, TX 78712

[g] Institut für Anorganische Chemie II, Universität zu Köln, Greinstr. 6,
50939 Köln, Germany.

January 22, 2007

Pure rotational transitions of silicon monosulphide (^{28}Si^{32}S) and its rare isotopic species have been observed in their ground as well as vibrationally excited states by employing Fourier transform microwave (FTMW) spectroscopy of a supersonic molecular beam at centimetre wavelengths (13−37 GHz) and by using long-path absorption spectroscopy at millimetre and submillimetre wavelengths (127−925 GHz). The latter measurements include 91 transition frequencies for ^{28}Si^{32}S, ^{28}Si^{33}S, ^{28}Si^{34}S, ^{29}Si^{32}S and ^{30}Si^{32}S in $v = 0$, as well as 5 lines for ^{28}Si^{32}S in $v = 1$, with rotational quantum numbers $J'' \leq 52$. The centimetre-wave measurements include more than 300 newly recorded lines. Together with previous data they result in almost 600 transitions ($J'' = 0$ and 1) from all twelve possible isotopic species, including ^{29}Si^{36}S and ^{30}Si^{36}S, which have fractional abundances of about 7×10^{-6} and 4.5×10^{-6}, respectively. Rotational transitions were observed from $v = 0$ for the least abundant isotopic species to as high as $v = 51$ for the main species. Owing to the high spectral resolution of the FTMW spectrometer, hyperfine structure from the nuclear electric quadrupole moment of ^{33}S was resolved for species containing this isotope, as was much smaller nuclear spin-rotation splitting for isotopic species involving ^{29}Si. By combining the measurements here with previously published microwave and infrared data in one global fit, an improved set of spectroscopic parameters for SiS has been derived which include several terms describing the breakdown of the Born-Oppenheimer approximation. With this parameter set, highly accurate rotational frequencies for this important astronomical molecule can now be predicted well into the terahertz region.

1 Introduction

More than 130 molecules have been detected in the interstellar medium or in circumstellar shells.[1, 2] Nearly 10 % of these contain silicon, despite the refractory nature of silicon and many Si-containing molecules.[2, 3] Shock vapourisation has been proposed as the mechanism which releases silicon compounds from the grains into the interstellar gas.[4] Many Si-bearing molecules have been detected in the shell of the nearby carbon-rich asymptotic giant branch star IRC+10216 (CW Leo).[3] Silicon monosulphide, SiS, is one of the more abundant molecules in this source,[5, 6] where it is thought to be the progenitor for much of the Si chemistry.[4] However, SiS has also been observed toward massive star-forming regions such as Sagittarius B2 near the Galactic centre.[5] A total of seven rare isotopic species of SiS, including two doubly-substituted ^{29}Si^{34}S, ^{30}Si^{34}S[7] and ^{28}Si^{36}S[8] have now been detected in space, as have higher rotationally ($J = 20 - 19$[9, 10]) and vibrationally ($v = 3$[7]) excited transitions. Maser activity in the ground vibrational state of ^{28}Si^{32}S was detected toward IRC+10216 rather early for the $J = 1-0$ transition[11] and very recently for higher-J transitions.[12] Even rovibrational spectra have been recorded toward this carbon-rich star.[13]

Hoeft et al. studied the pure rotational spectrum of SiS in the laboratory in a series of papers

around 40 years ago.[14, 15, 16, 17] Transitions from the ground and excited vibrational states of normal $^{28}Si^{32}S$[14, 15] and four singly-substituted species containing $^{29,30}Si$ and $^{33,34}S$ were reported.[14, 16, 17] The dipole moment[15, 18] and the ^{33}S quadrupole coupling constant[16] in the ground vibrational state were also determined, as well as the effect of the breakdown of the Born-Oppenheimer approximation.[17, 19] Rovibrational transitions of SiS were subsequently measured by Fourier transform emission spectroscopy[20] and by diode laser infrared spectroscopy.[21] Both studies involved the four most abundant isotopic species (see Table 1) and went to fairly high rotational ($J_{\max} = 139$[20] or 150[21]) and vibrational quantum numbers ($v_{\max} = 7$[20] or 10[21]).

A few years ago, several of us measured the two lowest rotational transitions of the three most abundant isotopic species of silicon monosulphide, $^{28}Si^{32}S$, $^{29}Si^{32}S$ and $^{28}Si^{34}S$.[22] The use of a pulsed molecular beam Fourier transform microwave (FTMW) spectrometer equipped with an electric discharge nozzle permitted the detection of rotational transitions in highly excited vibrational levels up to $v = 51$ for $^{28}Si^{32}S$, which corresponds to an energy of about 30000 cm^{-1}, nearly 60 % of the dissociation limit.

The present investigation extends previous FTMW measurements to all 12 stable SiS isotopic species. Silicon possesses three naturally occurring isotopes, ^{28}Si, ^{29}Si and ^{30}Si, with relative abundances of 0.922, 0.047 and 0.031, respectively, while four isotopes occur for sulphur, ^{32}S, ^{33}S, ^{34}S and ^{36}S, with abundances of 0.95, 0.0075, 0.043 and 0.00015, respectively.[23] Each isotopic species has been detected in natural abundance, including $^{29}Si^{36}S$ and $^{30}Si^{36}S$ with fractional abundances of about 7×10^{-6} and 4.5×10^{-6}, respectively (see Table 1). A by-product of the present work is the determination of the ^{29}Si and ^{33}S hyperfine structure (hfs) as a function of vibrational excitation.

Even though the lower rotational transitions of SiS have been fairly accurately determined from previous studies (uncertainties of 2 kHz[22] or only a few kilohertz[17]), frequency predictions in the millimetre-wave and submillimetre-wave bands have to be handled with caution, because these are extrapolated from measurements which are quite limited in rotational excitation − to only $J = 2 - 1$ or possibly $3 - 2$. Inclusion of the infrared transitions[20, 21] only slightly improves predictions of the rotational lines because the infrared data have large uncertainties (0.5×10^{-3} cm^{-1} or ≈ 15 MHz at best). For these reasons, we have recorded rotational spectra of the five most abundant isotopic species of SiS, including transitions within the $v = 1$ excited vibrational state for $^{28}Si^{32}S$, up to almost 1 THz to high accuracy − to better than 1 ppm − so that astronomical observations with the existing APEX (Atacama Pathfinder EXperiment) or SMA (Sub-Millimeter Array) instruments or the upcoming Herschel Space Observatory, SOFIA (Stratospheric Observatory For Infrared Applications) or ALMA (Atacama Large Millimeter Array) can be undertaken with precise laboratory support.

2 Experimental details and observed spectra

Submillimetre-wave transitions of SiS were studied in Köln using the Cologne Terahertz Spectrometer, which is described in detail elsewhere.[24] Phase-locked backward-wave oscillators were used as sources and a liquid helium cooled hot-electron InSb bolometer as detector. The 3 m long absorption cell was kept at room temperature. Di(*t*-butylsulfanyl)silane, $((CH_3)_3CS)_2SiH_2$,[25, 26] was subjected to a flash pyrolysis in an effort to record rotational spectra of silanethione, H_2SiS. While no transitions of this molecule were detected, strong lines of SiS, a plausible decomposition product, were observed. Transitions were recorded between 399 and 923 GHz for $^{28}Si^{32}S$ in its ground vibrational state. Excited $v = 1$ transitions as well as ground state transitions of $^{28}Si^{34}S$, $^{29}Si^{32}S$ and $^{30}Si^{32}S$ were recorded in the frequency range 827−925 GHz. These frequencies are well above the Boltzmann peak at 300 K, which falls near 580 GHz.

Millimetre- and submillimetre-wave transitions of SiS in the ground vibrational state were observed in Bologna in a negative glow discharge cell[27] in the frequency range 127−743 GHz for $^{28}Si^{32}S$ with a source modulation millimetre wave spectrometer.[28] Transitions of $^{29}Si^{32}S$, $^{30}Si^{32}S$, $^{28}Si^{33}S$ and $^{28}Si^{34}S$ were recorded between 335 and 582 GHz. The SiS molecules were produced directly in the absorption cell by a DC glow discharge through a mixture of silicon tetrachloride, $SiCl_4$, and hydrogen sulphide, H_2S, using Ar as buffer gas. Optimal conditions were attained using 20 mTorr of Ar, 2 mTorr of $SiCl_4$ and 1 mTorr of H_2S. The discharge current was in the range 30−60 mA, and the cell was kept at room temperature. Phase-locked Gunn oscillators working in the frequency region 55−115 GHz were used as primary radiation sources and the sub-millimetre investigations were carried out with harmonic generation. Source frequency modulation at 16.7 kHz was applied, and the signal was demodulated at $2f$ by a lock-in amplifier, thus obtaining the second derivative of the actual line profile. A liquid helium-cooled InSb hot electron bolometer served as detector.

Only a few transitions of $^{28}Si^{32}S$ were recorded both in Köln and in Bologna. The measurement with the smaller uncertainty was used in the present analysis; for the few lines with the same uncertainties, the average frequency was used.

Transition frequencies with assignments, uncertainties, and residuals between the observed frequency and those calculated from the final set of spectroscopic parameters are given for $^{28}Si^{32}S$, $v = 0$ in Table 2. The complete line list is available as supplementary material as well as in the Cologne Spectroscopy Data section of the Cologne Database for Molecular Spectroscopy, CDMS.[1, 2]

The $J'' = 0$ and 1 transitions of the nine remaining isotopic species of SiS not studied in Ref. [22] were recorded in at least the ground vibrational state with the same pulsed molecular

beam FTMW spectrometer and discharge nozzle [29] as previously employed. As before, a mixture of approximately 0.2 % SiH_4 and 0.05 % CS_2 was subjected to a 1.4 kV discharge. It is worth noting that the yield of SiS is remarkably high by this method: based on intensity measurements relative to a gas sample containing a known fractional abundance of a stable molecule in Ne (1% OCS), more than 10 % of the silane precursor is converted to SiS. For the comparatively abundant $^{30}Si^{32}S$, rotational transitions in vibrational states up to $v = 31$ were measured, while only those in $v = 0$ were detected for $^{29}Si^{36}S$ and $^{30}Si^{36}S$, owing to their much lower fractional abundances (Table 1). Some very high-v, $J'' = 0$ transitions of $^{28}Si^{32}S$ and $^{29}Si^{32}S$, which were not recorded in the previous study, were measured here for the first time. Transitions of $^{28}Si^{33}S$ for $v \leq 2$ are given in Table 3 to demonstrate the centimetre-wave dataset.

3 Determination of spectroscopic parameters

The ro-vibrational energy levels of a diatomic molecule AB can be represented by the Dunham expression:

$$E(v, J) = \sum_{i,j} Y_{ij}(v + 1/2)^i J^j (J + 1)^j \tag{1}$$

where the Y_{ij} are the Dunham parameters. Watson has shown that several isotopic species of AB can be fit jointly by constraining the Y_{ij} to

$$Y_{i,j} = U_{i,j} \left(1 + \frac{m_e \Delta_{ij}^{\mathrm{A}}}{M_{\mathrm{A}}} + \frac{m_e \Delta_{ij}^{\mathrm{B}}}{M_{\mathrm{B}}} \right) \mu^{-(i+2j)/2} \tag{2}$$

where $U_{i,j}$ is isotope invariant, m_e is the mass of the electron, μ is the reduced mass of AB, M_{A} is the mass of atom A, and Δ_{ij}^{A} is a Born-Oppenheimer breakdown term.[30] $U_{ij}\mu^{-(i+2j)/2}\Delta_{ij}^{\mathrm{A}} m_e/M_{\mathrm{A}}$ is sometimes abbreviated as δ_{ij}^{A}. Moreover, it is noteworthy that both Δ_{ij}^{A} and δ_{ij}^{A} are defined negatively in some papers. Obviously, Δ_{ij}^{B} and δ_{ij}^{B} are defined equivalently.

Both Si and S only have one isotope with a non-zero nuclear spin, ^{29}Si ($I = 1/2$) and ^{33}S ($I = 3/2$), which gives rise to hyperfine structure in SiS from either electric quadrupole coupling (^{33}S), magnetic spin-rotation coupling (^{29}Si), or both, that is readily resolved at high spectral resolution. For $^{29}Si^{33}S$, the hfs may be slightly more complicated because of scalar (normally denoted by the parameter J) and tensorial nuclear spin-nuclear spin coupling (S). For fairly light nuclei with small magnetic moments, the scalar contribution is typically negligible, and the tensorial contribution is dominated by a term that can be derived from the structure.[31] For SiS, this term amounts to 0.256 kHz − a value that is almost negligible in the present analysis − and therefore fixed in the fit. The quadrupole coupling parameters

eQq_{ij} scale with $\mu^{-(i+2j)/2}$, as do S_{ij} and J_{ij} while the spin-rotation parameters C_{ij} scale with $\mu^{-(i+2j+2)/2}$.

The atomic masses were taken from a recent compilation of Audi et al.[32] The precision of the atomic masses has improved over the past few decades to the point that they are usually not a limiting factor in analyses of diatomic spectra, but this was not the case in early studies of SiS.[17, 19]

Together with the new data, nearly all previously published data have been folded into the present global fit. The two infrared spectroscopic investigations [20, 21] are somewhat complementary, since the latter [21] extends to higher J and v while the former [20] has a greater coverage in J, particularly for lower vibrational states.

Most of the rotational transitions reported by Hoeft et al.[14, 15, 16, 17] have been remeasured in our first FTMW study on SiS,[22] but a few transitions with $J'' = 2$ have been retained in the present fit. A small number of transitions from Ref. [22] have been reanalysed because measured frequencies differed from those calculated from the best-fit parameters by more than 2.5 times their measurement uncertainties.

As indicated in Eq. 2, in theory, one isotopic substitution for each atom should be sufficient to determine all of the required Born-Oppenheimer breakdown terms; additional substitutions simply yield redundant information, except, for those, such as ^{28}Si^{33}S which also provide ^{33}S hyperfine parameters. In practice, however, multiple substitution of each atom is desirable to reduce correlations between the parameters and their Born-Oppenheimer breakdown terms, and redundancy has the beneficial effect of reducing calculated uncertainties. In addition, it provides a consistency check on the data. In fact, the very small hyperfine splitting of the $J = 2-1$ transition of ^{29}Si^{32}S which was close to the resolving capabilities of our spectrometer, were interpreted slightly differently in the present study compared with the previous one.[22] Instead of assigning the strong line of a two line pattern to the overlap of the two strong $\Delta F = +1$ components and the weak one to the weak $\Delta F = 0$ component, the present, more extensive data set is consistent with assigning the two lines to the two strong $\Delta F = +1$ components while the $\Delta F = 0$ component is likely too weak to be observed. Relative intensities of lines in FTMW spectroscopy should be viewed with caution, especially so in the case of closely spaced lines.

All fits and predictions have been performed employing Pickett's SPFIT and SPCAT programmes.[33] The input data were weighted inversely proportional to the measurement uncertainties, as is usually the case. The adequacy of these uncertainties was tested by checking how well various subsets of the data could be reproduced. Such tests are particularly important for an extensive

and diverse data set as the present one. The choice of spectroscopic parameters was rather straightforward from the previous FTMW study.[22] Transitions of $^{28}Si^{32}S$ in the highest three vibrational states ($v = 49 - 51$) proved to be difficult to reproduce. A trial fit with Y_{71} included in the fit reduced the residuals considerably, but its value was deemed to be too big: $(-5.9 \pm 0.5) \times 10^{-12}$ MHz; moreover, it also resulted in sizable changes in the lower-order Y_{n1} parameters. Trial fits with fixed values for Y_{71} indicated that a value of around -0.5×10^{-12} MHz is required to account for the residuals of the high-v transitions. This value was kept fixed in the final fit.

Three infrared transitions from Ref. [21] were omitted from the fit because their residuals exceeded three times their measurements uncertainties and because the omission had only a negligible effect on the derived parameters. Three other R-branch transitions with $v = 3 - 2$ and $J'' \approx 150$ had also large residuals; we have doubled their measurement uncertainties in the present analysis.

The Born-Oppenheimer corrections for Y_{11} were used for the first time while those for Y_{02} were omitted because they were not determined with significance, they appeared to be too large in magnitude, and they had only a negligible effect on the quality of the fit. The parameter Y_{32} as well as the hyperfine terms C_{10} were not used in the final fits for similar reasons. As discussed in section 4, Y_{13} was retained in the fit even though it appeared to be rather large with respect to Y_{03}.

The final set of spectroscopic parameters for the $^{28}Si^{32}S$ is given in Table 4. The rms error is 0.753 for the global fit, an indication that the input data are generally well reproduced to within the experimental uncertainties. The rms errors for the individual subsets vary between 0.502 and 0.984.

4 Discussion

Almost all of the spectroscopic parameters included in the final fit have been determined with significance. The Born-Oppenheimer breakdown terms δ_{10}^{S} and δ_{11}^{Si} have been included despite their large uncertainties relative to their values because their uncertainties are comparable in magnitude to those of δ_{10}^{Si} and δ_{11}^{S}, respectively.

The use of Y_{13} in addition to Y_{03} requires special consideration, as both are of similar magnitude, and Y_{03} is only determined to 25 %. The comparison of the decrease in the series Y_{0n} ($n \leq 3$) with that in the Y_{1n} reveals that it is not Y_{13} that is particularly large in magnitude, rather Y_{03} is particularly small. In fact, these two parameters were already in the fit of Frum

et al. [20] with rather similar values.

The spectroscopic parameters determined here agree well with those obtained previously, [17, 19, 20, 21, 22] even though the present dataset is much more extensive, e. g. there are more than twice as many pure rotational data than in Ref. [22], see Table 1. In addition, the uncertainties of the parameters are generally much smaller than in the previous work; e. g. the parameter uncertainties of Y_{01}, Y_{02} and Y_{03} were reduced by factors of 5, 20 and 6, respectively, despite inclusion of additional parameters, such as Y_{13}.

The reassignment of the hyperfine structure in the $J = 2-1$ transitions of ^{29}Si^{32}S in the present analysis compared with Ref. [22] has a small, but non-negligible effect on the centre frequencies of these transitions which, in turn, affects predominantly U_{01} and $\Delta_{01}^{\mathrm{Si}}$. The reassignment increases the value for C(Si) in magnitude from -10.39 ± 0.21 kHz to -14.44 ± 0.02 kHz. The agreement between the previous and the present value for Y_{01} is very good, as is that of most other parameters.

The Born-Oppenheimer breakdown terms Δ_{10} and Δ_{01} derived for SiS in the present investigation and in previous ones are compared in Table 5. The agreement is generally fairly good. Rather remarkable is the agreement of the present Δ_{01} with those from Ref. [19]. The uncertainties of the Δ_{10} from Ref. [20] are smaller than the present ones because their uncertainties have been derived for an ideal rms error of 1.0, as is quite common, whereas in the present work no such scaling of the parameter uncertainties was made.

Among the Born-Oppenheimer breakdown terms the ones for $Y_{01} \approx B_e$ are usually the ones determined best while others often were obtained without or with little significance. It is therefore not surprising that only these terms have been discussed in detail. According to Watson,[30] these terms contain three contributions, (i) a term that originates in the Dunham formalism and is usually very small, (ii) a diabatic (or non-adiabatic) term that is proportional to the dipole moment μ and the molecular g-value g_J, and finally, (iii) an adiabatic term that is derived by subtracting the two former contributions from the experimental value. Tiemann et al.[19] discussed Born-Oppenheimer breakdown terms for two groups of molecules with ten valence electrons consisting of C to Pb and O to Te as one atom and of Ga to In and F to I as the other. They found that the adiabatic contribution is more a property that depends on the respective atom than on the particular molecule. Moreover, its value is negative and usually small in magnitude for light or fairly light atoms, but it may have a large one for heavier atoms such as Sn and In, and even more so for Pb and Tl because of the finite nuclear sizes.[34, 35] This conclusion has been corroborated by recent theoretical calculations.[36]

Born-Oppenheimer breakdown terms for SiS and related molecules are shown in Table 6. The

Δ_{10} values are comparatively small in magnitude, and the three available values for the respective A atom are all positive. In contrast, there seems to be no clear trend in the Δ_{11}.

The SiS equilibrium bond lengths r_e have been calculated for the various isotopic species according to $r_e^2 \times B_e \times \mu = X$ and are given in Table 7. Here B_e is the equilibrium rotational constant derived from the Y_{01}, μ is the reduced mass as above, and $X = 505379.0094 \pm 0.0034$ amu MHz Å^2 is the conversion constant with 1 Å = 100 pm. The value of X has recently been reevaluated from the Compton wavelength of the proton, the mass of the proton and the speed of light.[37, 38] The bond distance in the Born-Oppenheimer approximation is evaluated according to $r_e^2 \times U_{01} = X$. It should be noted that B_e is slightly different from Y_{01}[39]. In the case of ^{28}Si^{32}S B_e is 2.454 ± 0.033 kHz larger than the Y_{01} value. The difference given by Tiemann et al.,[17] 4 ± 3 kHz, is less accurate than the present value, but compatible with it within error bars. In contrast, 19 ± 2 kHz as deduced from Birk and Jones[21] appears to be too large.

The value for r_e is independent of the isotopic species in the Born-Oppenheimer approximation. The breakdown of this approximation leads to bond lengths that are longer by about 6 fm, a relative difference of $\sim 5 \times 10^{-5}$, with isotopic differences in the bond length that are one to two orders of magnitude smaller, as can be seen in Table 7. The difference between B_e and Y_{01} corresponds to a change of only 26 atto metre in the interatomic distance, which is essentially the same as the uncertainty of the bond length in the Born-Oppenheimer approximation, but about an order of magnitude larger than the uncertainties of the bond lengths when the breakdown of that approximation has been taken into account.

The equilibrium nuclear quadrupole coupling parameters eQq_{00} of ^{33}S in CS and SiS in Table 8 are rather similar, as one might expect for related molecules. The vibrational corrections eQq_{10} and eQq_{20} of the latter molecule are smaller than those of the former because SiS is much heavier. However, the ratio R of the reduced nuclear quadrupole coupling terms $eQq_{ij}\mu^{(i+2j)/2}$ is decreased slightly, and, the vibrational corrections relative to the vibrational energy are increasing slightly for SiS with respect to CS, as might be expected because the SiS molecule is less rigid than CS.

The spin-rotation coupling parameter C is the sum of an electronic part $C_{\rm el}$ and a nuclear part $C_{\rm nucl}$; the latter can be calculated directly from the geometrical structure, as described e. g. in Ref. [31]. $C_{\rm el}$ is proportional to the rotational constant B_e, the magnetic g factor of the nucleus and the paramagnetic shielding σ_p at the nucleus. As an excited state property, it is σ_p and thus also $C_{\rm el}$ that is a challenge for *ab initio* calculations. The value of σ_p can be obtained as a sum in which each summand is proportional to $\langle r^{-3} \rangle$, which is the expectation value over electron coordinates on valence orbitals of the respective atom, an occupation or weighting number and inversely proportional to the energy of excited singlet states in the case of a singlet molecule;

see e. g. in Ref. [31].

The values for C, C_{nucl}, C_{el} and σ_p for the molecules CS, SiS and SiO are given in Table 9. Trial fits with the vibrational corrections C_{10} increased the uncertainties of C by about 50 %, with essentially no change in the value for Si and a decrease in the value for S by 0.14 kHz, slightly more than the increased uncertainty. The effects on the derived paramagnetic shielding values are of similar relative magnitude.

The paramagnetic shielding at S is very similar in CS and SiS. The small differences are likely caused by the lower-lying electronic states of SiS relative to those of CS. The difference in the shielding is more pronounced at the other nucleus. The increase in $\langle r^{-3} \rangle$ from C to Si is responsible for much of this difference, as may be deduced from calculated $\langle r^{-3} \rangle$ values.[42] The remaining difference is caused by different occupation or weighting numbers and appears to be about twice as large as that of the S nuclei. The shielding at Si is smaller in SiO than in SiS, as expected, but the magnitude of this difference is quite large. It can largely be accounted for by the lower excited electronic states of SiS relative to those of SiO: the two lowest singlet states are near 29000 cm^{-1} in SiS[43] while the two lowest and corresponding states in SiO are near 39000 cm^{-1}.[44] ^{17}O hyperfine parameters for the electronic ground state of SiO are presently not available.

5 Conclusion

Very accurate rotational transition frequencies of all 12 stable SiS isotopic species are now available in the microwave region. They cover very high vibrational states for the more abundant species. The ^{33}S nuclear electric quadrupole coupling parameter and vibrational corrections have been determined along with nuclear magnetic spin-rotation parameters for ^{29}Si and ^{33}S; the values derived here compare favourably with those of related molecules. Rotational transition frequencies exceeding 100 GHz and reaching almost 1000 GHz have been determined for the first time in the course of the present work for several isotopic species. The improved spectroscopic parameters permit reliable predictions of rotational transitions well into the terahertz region. The predicted uncertainties of the ground state rotational transitions of ^{28}Si^{32}S reach uncertainties of $\sim$ 7, 150 and 830 kHz at 1.0, 1.5 and 2.0 THz, respectively, which corresponds to J'' of 54, 82 and 111. These uncertainties are almost irrespective of the isotopic species or vibrational state considered. By comparison, the Boltzmann peak of the SiS pure rotational spectrum occurs near 0.58 THz at 300 K. We estimate that actual transitions are found not farther away from the predicted frequencies than three to ten times of the predicted uncertainties as long as J is smaller than 120 or the frequency is below 2.15 THz.

Predictions of the rotational spectra of various SiS isotopic species, including those for excited vibrational states as well as rovibrational transitions for the more abundant ones, will be available in the catalogue section of the CDMS.[1, 2] Knowledge of the permanent dipole moment and the vibrational transition moments are necessary to derive SiS column densities or abundances in space from the pure rotational or the rovibrational spectrum, respectively. The permanent electric dipole moment μ of SiS has been determined experimentally in the ground vibrational state with moderate accuracy to be 1.73 ± 0.06 D[15] or 1.74 ± 0.07 D.[18] Vibrational and rotational corrections to the dipole moment μ_{10} and μ_{01} are only available from *ab initio* calculations and are about -12.2 mD and -5 μD, respectively, with μ_e being positive.[45] The calculations should be viewed with some caution as the observed magnitude of μ_{10} for SiO[46] is about 50 % larger than the calculated one.[45] Taking into account the experimental μ_{10} values for CS,[47] SiO and GeO[46] as well as the derived value for CO,[48] the SiS value is probably more like -17.5 ± 1.0 mD, which is, as in the SiO case, about 50 % larger than the calculated one. The transition dipole moments of the $v = 1 - 0$ and $v = 2 - 0$ vibrational bands have been estimated to be 130 and -6.3 mD, respectively.[49]

6 Acknowledgements

The investigations in Köln were supported by the Deutsche Forschungsgemeinschaft (DFG) *via* Grant SFB 494. Additional support by the Ministry of Science and Technology of the Land Nordrhein-Westfalen (NRW) is acknowledged. The work in Cambridge is supported by the National Science Foundation, Grant CHE−0353693. H. G. acknowledges additional support by the Robert A. Welch foundation through a grant to J. F. Stanton at the University of Texas. L. B. and C. D. E. thank MIUR and University of Bologna (Funds for Selected Research Topics) for financial support.

References

[1] H. S. P. Müller, F. Schlöder, J. Stutzki and G. Winnewisser, *J. Mol. Struct.*, 2005, **742**, 215−227.

[2] Internet address: http://www.ph1.uni-koeln.de/vorhersagen/ ; short-cut: www.cdms.de .

[3] M. C. McCarthy, C. A. Gottlieb and P. Thaddeus, *Mol. Phys.*, 2003, **101**, 697−704.

[4] E. g. K. Willacy and I. Cherchneff, *Astron. Astrophys.* 1998, **330** 676−684.

[5] M. Morris, W. Gilmore, P. Palmer, B. E. Turner and B. Zuckerman, *Astrophys. J.*, 1975, **199**, L47−L51.

[6] J. H. Bieging and Q.-R. Nguyen, *Astrophys. J.*, 1989, **343**, L25−L28.

[7] J. Cernicharo, M. Guélin and C. Kahane, *Astron. Astrophys. Suppl. Ser.* 2000, **142** 181−215.

[8] R. Mauersberger, U. Ott, C. Henkel, J. Cernicharo and R. Gallino, *Astron. Astrophys.* 2004, **426** 219−227.

[9] L. W. Avery, T. Amano, M. B. Bell, P. A. Feldman, J. W. C. Johns, J. M. MacLeod, H. E. Matthews, D. C. Morton, J. K. G. Watson, B. E. Turner, S. S. Hayashi, G. D. Watt and A. S. Webster, *Astrophys. J. Suppl. Ser.* 1992, **83** 363−385.

[10] T. D. Groesbeck, T. G. Phillips and G. A. Blake, *Astrophys. J. Suppl. Ser.* 1994, **94** 147−162.

[11] C. Henkel, H. E. Matthews and M. Morris, *Astrophys. J.*, 1983, **267**, 184−190.

[12] J. P. Fonfría Expósito, M. Agúndez, B. Tercero, J. R. Pardo and J. Cernicharo, *Astrophys. J.*, 2006, **646**, L127−L130.

[13] R. J. Boyle, J. J. Keady, D. E. Jennings, K. L. Hirsch and G. R. Wiedemann, *Astrophys. J.*, 1994, **420**, 863−868.

[14] J. Hoeft, *Z. Naturforsch.*, 1965, **20a**, 1327−1329.

[15] J. Hoeft, F. J. Lovas, E. Tiemann and T. Törring, *Z. Naturforsch.*, 1969, **24a**, 1422−1423.

[16] J. Hoeft, F. J. Lovas, E. Tiemann and T. Törring, *J. Chem. Phys.*, 1970, **53**, 2736−2743.

[17] E. Tiemann, E. Renwanz, J. Hoeft and T. Törring, *Z. Naturforsch.*, 1972, **27a**, 1566−1570.

[18] A. N. Murty and R. F. Curl, Jr., *J. Mol. Spectrosc.*, 1969, **30**, 102−110.

[19] E. Tiemann, H. Arnst, W. U. Stieda, T. Törring and J. Hoeft, *Chem. Phys.*, 1982, **67**, 133−138.

[20] C. I. Frum, R. Engleman, Jr., and P. F. Bernath, *J. Chem. Phys.*, 1990, **93**, 5457−5461.

[21] H. Birk and H. Jones, *Chem. Phys. Lett.*, 1990, **175**, 536−542.

[22] M. E. Sanz, M. C. McCarthy and P. Thaddeus, *J. Chem. Phys.*, 2003, **119**, 11715−11727.

[23] J. K. Böhlke, J. R. de Laeter, P. De Bièvre, H. Hidaka, H. S. Peiser, K. J. R. Rosman and P. D. P. Taylor, *J. Phys. Chem. Ref. Data*, 2005, **34**, 57−67.

[24] G. Winnewisser, A. F. Krupnov, M. Y. Tretyakov, M. Liedtke, F. Lewen, A. H. Saleck, R. Schieder, A. P. Shkaev, and S. V. Volokhov, *J. Mol. Spectrosc.*, 1994, **165**, 294−300.

[25] D. Brandes, *J. Organomet. Chem.*, 1976, **105**, C1−C5.

[26] M. Hoverath, PhD Dissertation, Universität zu Köln, 1999.

[27] L. Dore, C. Degli Esposti, A. Mazzavillani and G. Cazzoli, *Chem. Phys. Lett.*, 1999, **300**, 489−492.

[28] G. Cazzoli and L. Dore *J. Mol. Spectrosc.*, 1990, **141**, 49−58.

[29] J.-U. Grabow, E. S. Palmer, M. C. McCarthy and P. Thaddeus, *Rev. Sci. Instr.*, 2005, **76**, Art.-No. 093106.

[30] J. K. G. Watson, *J. Mol. Spectrosc.*, 1973, **45**, 99−113.

[31] H. S. P. Müller and M. C. L. Gerry, *J. Chem. Phys.*, 1995, **103**, 577−583; and references therein.

[32] G. Audi, A. H. Wapstra and C. Thibault, *Nucl. Phys. A*, 2003, **729**, 337−676.

[33] H. M. Pickett, *J. Mol. Spectrosc.*, 1991, **148**, 371−377.

[34] E. Tiemann, H. Knöckel and J. Schlembach, *Ber. Bunsenges. Phys. Chem.*, 1982, **86**, 821−824.

[35] J. Schlembach and E. Tiemann, *Chem. Phys.*, 1982, **68**, 21−28.

[36] S. A. Cooke, M. C. L. Gerry and D. P. Chong, *Chem. Phys.*, 2004, **298**, 205−212.

[37] P. J. Mohr and B. N. Taylor, *Rev. Mod. Phys.*, 2005, **77**, 1−107.

[38] R. J. Le Roy, private communication, 2007.

[39] E. g. C. H. Townes and A. L. Schawlow, *Microwave Spectroscopy*, Dover Publications, New York, 1975, 3−14.

[40] T. George, W. Urban and A. Le Floch, *J. Mol. Spectrosc.*, 1994, **165**, 500−505.

[41] R. Gendriesch et al., unpublished.

[42] J. A. J. Fitzpatrick, F. R. Manby and C. M. Western, *J. Chem. Phys.*, 2005, **122**, Art.-No. 084312.

[43] S. M. Harris, R. A. Gottscho, R. W. Field and R. F. Barrow, *J. Mol. Spectrosc.*, 1982, **91**, 35−59.

[44] R. W. Field, A. Lagerqvist, and I. Renhorn, *J. Chem. Phys.*, 1977, **66**, 868−869.

[45] G. Maroulis, C. Makris, D. Xenides and P. Karamanis, *Mol. Phys.*, 2000, **98**, 481−491.

[46] J. W. Raymonda, J. S. Muenter and W. A. Klemperer, *J. Chem. Phys.*, 1970, **52**, 3458−3461.

[47] G. Winnewisser and R. L. Cook, *J. Mol. Spectrosc.*, 1968, **28**, 266−268.

[48] D. Goorvitch, *Astrophys. J. Suppl. Ser.*, 1994, **95**, 535−552.

[49] A. Lopez Piñeiro, R. H. Tipping and C. Chackerian, Jr., *J. Mol. Spectrosc.*, 1987, **125**, 184−187.

Table 1: Summary of the SiS data set used in the final fit showing the isotopic species and their relative abundances. The number of lines,[a] the maximum rotational $J_{\max}$ and vibrational quantum number $v_{\max}$ from previous (prev) investigations[17, 20, 21, 22] and from the present (new) one are also provided. Values for rotational and rovibrational data are given separately.

Species	Abundance	No. of lines[a]		$J_{\max}$		$v_{\max}$	
		prev	new	prev	new	prev	new
rotational data							
$^{28}Si^{32}S$	8.8×10^{-1}	101	49	3	51	51	51
$^{29}Si^{32}S$	4.5×10^{-2}	109	29	3	50	29	31
$^{30}Si^{32}S$	2.9×10^{-2}	2	70	3	53	1	33
$^{28}Si^{33}S$	6.9×10^{-3}	–	128	–	2	–	16
$^{29}Si^{33}S$	3.5×10^{-4}	–	41	–	2	–	3
$^{30}Si^{33}S$	2.3×10^{-4}	–	25	–	2	–	2
$^{28}Si^{34}S$	4.0×10^{-2}	62	15	3	51	31	0
$^{29}Si^{34}S$	2.0×10^{-3}	–	29	–	2	–	10
$^{30}Si^{34}S$	1.3×10^{-3}	–	22	–	2	–	6
$^{28}Si^{36}S$	1.4×10^{-4}	–	10	–	2	–	4
$^{29}Si^{36}S$	7.0×10^{-6}	–	4	–	2	–	0
$^{30}Si^{36}S$	4.5×10^{-6}	–	3	–	2	–	1
rovibrational data							
$^{28}Si^{32}S$		1451	–	150	–	10	–
$^{29}Si^{32}S$		361	–	107	–	4	–
$^{30}Si^{32}S$		289	–	101	–	4	–
$^{28}Si^{34}S$		348	–	104	–	4	–

[a] Overlapping hyperfine components have been counted as one line.

Table 2: Rotational transitions[a] (MHz) of $^{28}Si^{32}S$, $v = 0$, uncertainties Unc. (kHz), residuals[b] O−C (kHz) and source[c] of the measurement.

J''	Frequency	Unc.	O−C	Source
6	127 076.186	10	8	B
7	145 227.053	10	1	B
8	163 376.785	10	5	B
10	199 672.229	10	5	B
11	217 817.663	10	10	B
15	290 380.757	10	13	B
17	326 649.109	10	1	B
18	344 779.481	10	−11	B
19	362 907.164	10	9	B
20	381 031.954	10	3	B
21	399 153.731	10	−8	B, K
22	417 272.368	10	−7	B, K
23	435 387.701	10	−14	B
24	453 499.631	20	15	K
25	471 607.935	10	0	K
26	489 712.524	10	−4	B, K
27	507 813.258	10	5	B, K
28	525 909.965	5	−1	K
29	544 002.518	5	−6	K
30	562 090.777	5	−6	K
31	580 174.604	10	4	B
32	598 253.828	5	−4	K
33	616 328.337	10	2	B
35	652 462.584	10	0	B
36	670 522.052	10	10	B
37	688 576.198	10	−1	B
38	706 624.908	10	−3	B
39	724 668.036	10	2	B
40	742 705.423	10	−3	B
44	814 794.795	20	−16	K
45	832 801.405	25	10	K
46	850 801.384	5	−4	K
47	868 794.650	5	4	K
48	886 781.041	10	15	K

J''	Frequency	Unc.	O−C	Source
49	904 760.377	10	−8	K
50	922 732.579	5	0	K

[a] $J' - J''$.

[b] Observed frequency minus frequency calculated from the final set of spectroscopic parameters.

[c] B: Bologna, K: Köln.

Table 3: Rotational transitions[a] (MHz) of $^{28}Si^{33}S$, $v = 0$, 1 and 2, and residuals[b] O−C (kHz).

		$v = 0$		$v = 1$		$v = 2$	
J''	$F' - F''$	Frequency	O−C	Frequency	O−C	Frequency	O−C
0	0.5 − 1.5	17 895.651	0.9	17 809.245	−0.4	17 722.832	−0.1
0	2.5 − 1.5	17 897.869	0.5	17 811.413	−1.2	17 724.950	−1.9
0	1.5 − 1.5	17 900.591	1.9	17 814.074	1.1	17 727.549	−0.3
1	0.5 − 1.5	35 791.721	2.2	35 618.895	−1.8	35 446.053	−5.0
1	1.5 − 1.5	35 794.469	1.5	35 621.586	2.4	35 448.684	0.6
1	2.5 − 1.5	35 796.438	−2.6	35 623.508	−4.5	35 450.564	−4.5
1	3.5 − 2.5	35 796.447	−0.6	35 623.520	0.5	35 450.576	0.5
1	0.5 − 0.5	35 796.662	4.2	35 623.723	−1.4	35 450.773	−2.1
1	1.5 − 2.5	35 797.189	0.9	35 624.244	1.7	35 451.279	−1.8
1	2.5 − 2.5	35 799.162	0.8	35 626.170	−1.2	35 453.166	0.2
1	1.5 − 0.5	35 799.408	1.5	35 626.410	−1.2	35 453.400	−0.6

[a] $J' - J''$; uncertainties are 2 kHz throughout.
[b] Observed frequency minus frequency calculated from the final set of spectroscopic parameters.

Table 4: Spectroscopic parameters[a] (MHz) of $^{28}Si^{32}S$ determined from the global fit.

Parameter	Value
$U_{10}\mu^{-1/2} \times 10^{-6}$	22.473 483 2 (304)
$U_{10}\mu^{-1/2}\Delta_{10}^{Si} m_e/M_{Si}$	393.5 (189)
$U_{10}\mu^{-1/2}\Delta_{10}^{S} m_e/M_S$	−67.2 (207)
$Y_{10} \times 10^{-6}$	22.473 809 43 (261)[b]
Δ_{10}^{Si}	0.893 (43)[b,c]
Δ_{10}^{S}	−0.174 (54)[b,c]
$Y_{20} \times 10^{-3}$	−77.531 63 (93)
Y_{30}	30.909 (167)
$Y_{40} \times 10^{3}$	−203.8 (99)
$U_{01}\mu^{-1}$	9 100.078 47 (123)
$U_{01}\mu^{-1}\Delta_{01}^{Si} m_e/M_{Si}$	−0.248 65 (65)
$U_{01}\mu^{-1}\Delta_{01}^{S} m_e/M_S$	−0.292 41 (86)
Y_{01}	9 099.537 406 (74)[b]
Δ_{01}^{Si}	−1.393 5 (42)[b,c]
Δ_{01}^{S}	−1.872 8 (55)[b,c]
$U_{11}\mu^{-3/2}$	−44.165 497 (188)
$U_{11}\mu^{-3/2}\Delta_{01}^{Si} m_e/M_{Si}$	0.000 126 (114)
$U_{11}\mu^{-3/2}\Delta_{01}^{S} m_e/M_S$	0.000 990 (109)
Y_{11}	−44.164 381 (60)[b]
Δ_{11}^{Si}	−0.146 (132)[b,c]
Δ_{11}^{S}	−1.306 (144)[b,c]
$Y_{21} \times 10^{3}$	−0.999 8 (130)
$Y_{31} \times 10^{3}$	−0.223 76 (111)
$Y_{41} \times 10^{6}$	−2.854 (44)
$Y_{51} \times 10^{9}$	43.52 (81)
$Y_{61} \times 10^{9}$	−0.382 2 (56)
$Y_{71} \times 10^{12}$	−0.512[d]
$Y_{02} \times 10^{3}$	−5.967 274 (45)
$Y_{12} \times 10^{6}$	−5.512 6 (320)
$Y_{22} \times 10^{6}$	−0.112 52 (339)
$Y_{03} \times 10^{12}$	−33.0 (84)
$Y_{13} \times 10^{12}$	−19.20 (180)
$eQq_{00}(^{33}S)$	11.076 84 (148)
$eQq_{10}(^{33}S)$	−0.249 84 (62)
$eQq_{20}(^{33}S) \times 10^{3}$	1.125 (43)

Parameter	Value
$C_{00}(^{29}\mathrm{Si}) \times 10^3$	$-14.446\,9\,(219)$
$C_{00}(^{33}\mathrm{S}) \times 10^3$	$7.001\,(87)$
$S_{00} \times 10^3$	0.256^d

[a] Numbers in parentheses are one standard deviation in units of the least significant figures.
[b] Derived value.
[c] Unitless.
[d] Kept fixed in the fit, see section 3.

Table 5: Comparison of SiS Born-Oppenheimer breakdown terms[a] Δ_{10} and Δ_{01} with those from previous studies.

	This work	Ref. [19]	Ref. [20]	Ref. [21]	Ref. [22]
$\Delta_{10}^{\mathrm{Si}}$	0.893 (43)	–	1.31 (12)	0.929 (22)	0.890 (57)
Δ_{10}^{S}	−0.174 (54)	–	0.25 (16)	−0.257 (27)	−0.179 (70)
$\Delta_{01}^{\mathrm{Si}}$	−1.3935 (42)	−1.392 (59)	−1.45 (20)	−1.203 (52)	−1.097 (22)
Δ_{01}^{S}	−1.8728 (55)	−1.870 (64)	−1.91 (24)	−1.944 (58)	−1.772 (15)

[a] Numbers in parentheses are one standard deviation in units of the least significant figures.

Table 6: Comparison of Born-Oppenheimer breakdown terms[a] Δ_{10}, Δ_{01} and Δ_{11} for molecules AB with A = C, Si, and B = O, S.

	CO[b]	CS[c]	SiO[d]	SiS[e]
Δ_{10}^{A}	0.69463 (52)	0.7606 (115)	–	0.893 (43)
Δ_{10}^{B}	−0.16628 (26)	−0.6598 (346)	–	−0.174 (54)
Δ_{01}^{A}	−2.05603 (23)	−2.5434 (49)	−1.294 (35)	−1.3935 (42)
Δ_{01}^{B}	−2.09934 (28)	−2.3945 (34)	−2.0682 (95)	−1.8728 (55)
Δ_{11}^{A}	−1.641 (33)	−2.697 (130)	–	−0.146 (132)
Δ_{11}^{B}	−1.814 (32)	−0.985 (118)	−1.678 (58)	−1.306 (144)

[a] Numbers in parentheses are one standard deviation in units of the least significant figures.
[b] Ref. [40, 41].
[c] Ref. [1].
[d] Ref. [22].
[e] This work.

Table 7: SiS equilibrium bond lengths r_e (pm)[a] in the Born-Oppenheimer limit and values for the various isotopic species taking into account the deviations from the Born-Oppenheimer approximation.

Species	Value
SiS^{BO}	192.926 350 9 (261)
$^{28}Si^{32}S$	192.932 086 6 (24)
$^{29}Si^{32}S$	192.931 995 6 (24)
$^{30}Si^{32}S$	192.931 910 9 (24)
$^{28}Si^{33}S$	192.931 992 6 (24)
$^{29}Si^{33}S$	192.931 901 7 (24)
$^{30}Si^{33}S$	192.931 816 9 (24)
$^{28}Si^{34}S$	192.931 904 4 (23)
$^{29}Si^{34}S$	192.931 813 5 (23)
$^{30}Si^{34}S$	192.931 728 8 (23)
$^{28}Si^{36}S$	192.931 742 2 (25)
$^{29}Si^{36}S$	192.931 651 2 (25)
$^{30}Si^{36}S$	192.931 566 6 (25)

[a] Numbers in parentheses are one standard deviation in units of the least significant figures.

Table 8: Comparison of the ^{33}S quadrupole coupling parameters eQq_{ij} (MHz)[a] and the ratios R_{ij} of $eQq_{ij}\mu^{(i+2j)/2}$ for CS and SiS.

	CS[b]	SiS[c]	R
eQq_{00}	13.0265 (68)	11.07684 (148)	1.1760
eQq_{10}	−0.4007 (39)	−0.24984 (62)	0.976
$eQq_{20} \times 10^3$	2.50 (48)	1.125 (43)	0.82

[a] Numbers in parentheses are one standard deviation in units of the least significant figures.
[b] Ref. [1].
[c] This work.

Table 9: Comparison of nuclear spin-rotation coupling parameters C^a, their nuclear C_{nucl} and electronic contributions C_{el} (kHz) and paramagnetic shielding ${\sigma_p}^a$ (ppm) at the nucleus N for CS, SiS and SiO.

	N	C	C_{nucl}	C_{el}	σ_p
CS[b]	^{13}C	27.02 (59)	−5.53	32.55	−576.8 (105)
CS[b]	^{33}S	17.98 (25)	−0.63	18.61	−1079.4 (145)
SiS[c]	^{29}Si	−14.447 (22)	1.286	−15.733	−952.8 (13)
SiS[c]	^{33}S	7.001 (87)	−0.435	7.436	−1165.2 (136)
SiO[d]	^{29}Si	−21.40 (34)	1.97	−23.37	−591.1 (86)

[a] Numbers in parentheses are one standard deviation in units of the least significant figures.
[b] Ref. [1].
[c] This work.
[d] Ref. [22].

Fig. 1 Portion of the rotational spectrum of silicon monosulphide in the region of the $J = 1 - 0$, $v = 0$ transition of $^{29}Si^{33}S$ obtained in an integration time of 15 minutes. The transition is split into three widely spaced hyperfine components because of the quadrupole moment of the ^{33}S nucleus. The assignments of the ^{33}S hyperfine components are given. The line off scale is due to the $J = 1 - 0$, $v = 3$ transition of $^{29}Si^{32}S$. Each line is further split into four components, two because of the Doppler effect as the supersonic molecular beam travels parallel to the propagation of the microwave radiation and two because of small nuclear spin-rotation splitting ($\sim$ 18 kHz) due to the $I = 1/2$ spin of the ^{29}Si nucleus.

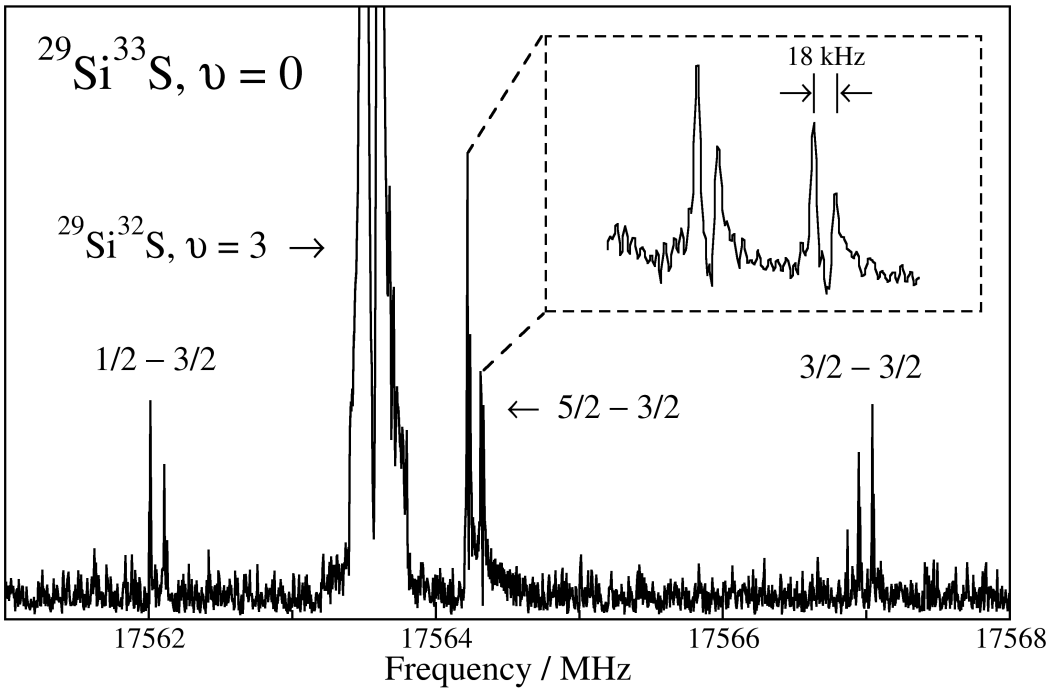

Figure 1: Portion of the rotational spectrum of silicon monosulphide in the region of the $J = 1 - 0$, $v = 0$ transition of $^{29}Si^{33}S$ obtained in an integration time of 15 minutes. The transition is split into three widely spaced hyperfine components because of the quadrupole moment of the ^{33}S nucleus. The assignments of the ^{33}S hyperfine components are given. The line off scale is due to the $J = 1 - 0$, $v = 3$ transition of $^{29}Si^{32}S$. Each line is further split into four components, two because of the Doppler effect as the supersonic molecular beam travels parallel to the propagation of the microwave radiation and two because of small nuclear spin-rotation splitting (~ 18 kHz) due to the $I = 1/2$ spin of the ^{29}Si nucleus.